Phytochemistry 177 (2020) 112452

Contents lists available at ScienceDirect

Phytochemistry

journal homepage: www.elsevier.com/locate/phytochem

Lipidomic analysis of diatoms cultivated with silica nanoparticles

Tomáš Řezanka [a,*], Michal Řezanka [b], Dana Mezricky [c], Milada Vítová [d]

[a] Institute of Microbiology of the Czech Academy of Sciences, Vídeňská 1083, 142 20, Prague, Czech Republic
[b] Department of Nanochemistry, Institute for Nanomaterials, Advanced Technologies and Innovation, Technical University of Liberec, Studentská 1402/2, 461 17, Liberec 1, Czech Republic
[c] Medical and Pharmaceutical Biotechnology, IMC University of Applied Sciences, Piaristengasse1, 3500, Krems, Austria
[d] Institute of Microbiology of the Czech Academy of Sciences, Centre Algatech, Laboratory of Cell Cycles of Algae, Novohradská 237, 379 81, Třeboň, Czech Republic

ARTICLE INFO

Keywords:
Diadesmis gallica
Diadesmidaceae
Navicula atomus
Naviculaceae
Diatoms
Silica nanoparticles
Phosphatidylsulfocholine
Fatty acids
Liquid chromatography-electrospray mass spectrometry

ABSTRACT

Polar lipids from the diatoms *Diadesmis gallica* and *Navicula atomus* were separated and their structures were determined using high resolution tandem MS HILIC-LC/ESI. This method allowed us to identify 34 classes of lipids, each containing dozens of molecular species, including regioisomers. The largest differences were found in two sulfur-containing lipids, sulfoquinovosyldiacylglycerol and phosphatidylsulfocholine caused probably by the remodeling of lipid species. These diatoms have been found to use several mechanisms to resolve growth in extreme environments, i.e. silica starvation. The presence of insoluble nano-SiO_2 leads to the replacement of cellular phospholipids with sulfolipids. Regioisomer ratios also vary depending on the concentration of nano-SiO_2 in the culture medium, i.e. the biosynthesis of polar lipids via the prokaryotic (plastidial) and/or eukaryotic (explastidial) pathways. Complex analyses of polar lipids using high resolution HILIC-LC/ESI-tandem, as used for diatoms, can also be used for other photosynthetic microorganisms.

1. Introduction

Diatoms (Bacillariophyceae = Diatomophyceae) are unicellular or colonial coccoid algae encased in a siliceous cell wall called a frustule. Both marine and freshwater diatoms contain fatty acids (FA) from C14 to C22, i.e. from myristic to docosahexaenoic acids (Cramer et al., 2011), and the FA content is usually up to 20% dry weight, but can also be up to 65% of the dry weight of cells (Taguchi et al., 1987). They have also been examined for use as a feedstock for biofuel (Popovich et al., 2012). The content of fatty acids in the genus *Navicula* is very variable, for example, in *N. gregaria* the content of palmitoleic acid was more than half of the total FA (Anisimov et al., 2011) and the eicosapentaenoic acid content in the phospholipid fraction was over 27% of total FA. In *N. pelliculosa*, palmitoleic and eicosapentaenoic acids were identified as the majority, but also hexadecatrienoic acid (18.3% of total FA) (Bell et al., 2012) Also in *N. perminuta*, palmitic, palmitoleic, and eicosapentaenoic acids were identified as the major FAs, while polyunsaturated C16 and C18 were minor components (Schaub et al., 2017). Conversely (Lang et al. (2011) found predominantly palmitic, palmitoleic, and hexadecatrienoic acids in the genus *Navicula*, but not C20 or longer polyunsaturated fatty acids (PUFA) such as arachidonic, eicosapentaenoic, and docosahexaenoic acids.

The polar lipid fraction of diatoms mainly consists of monogalactosyldiacylglycerol (MGDG), digalactosyldiacylglycerol (DGDG), sulfoquinovosyldiacylglycerol (SQDG), phosphatidylcholine (PC), phosphatidylinositol (PI), phosphatidylglycerol (PG) and other, minor lipids (Stonik and Stonik, 2015). Some diatoms contain less common sulfolipids, such as phosphatidylsulfocholine (PSC), i.e. the sulfonium analog of PC, 1-deoxyceramide-1-sulfate or 24-methylene cholesterol sulfate.

One of the first papers describing diatom lipids, including polar lipids from the fresh water diatom *N. pelliculosa,* was published over 50 years ago (Kates and Volcani, 1966). Phosphatidic acid (PA), phosphatidylethanolamine (PE), phosphatidylserine (PS), cardiolipin (CL, i.e. diphosphatidylglycerol), PC, PI, PG, DGDG, MGDG and SQDG, including minor polar lipids such as phosphatidyl-*N*-methyl ethanolamine (MMPE) or three sulfolipids were identified based on TLC of native lipids, incorporation of labeled compounds ($^{14}CO_2$, $^{35}SO_4^{2-}$ and $H^{32}PO_4^{2-}$), deacylation of lipids and subsequent paper chromatography of water-soluble compounds originating from the head of polar lipids. One of them was later identified as PSC (Bisseret et al., 1984). Another method used for the determination of PC and PSC mixtures was ammonia desorption chemical ionization mass spectrometry (Bisseret et al., 1985).

* Corresponding author.
E-mail address: rezanka@biomed.cas.cz (T. Řezanka).

https://doi.org/10.1016/j.phytochem.2020.112452
Received 7 April 2020; Received in revised form 16 June 2020; Accepted 20 June 2020

Total lipids of the benthic diatom *N. perminuta* were separated and quantified by silica gel HPLC (Schaub et al., 2017). The major neutral lipids such as triacylglycerol (TAG) and free fatty acids (FFA), including minor diacylglycerols (DAG) and cholesterol were analyzed. Commonly occurring polar lipids such as SQDG, DGDG, MGDG, ceramides, PI, lysophosphatidylcholine (LPC), PE, and PC were also identified. Further, polar lipids with unknown structures, i.e. two major and three minor peaks were also noted.

Based on the above examples, it is obvious that the content of individual FA and lipids, including polar lipids (phospholipids and/or glycolipids) of diatoms is very variable. Depending on the different cultivation conditions, e.g. temperature of cultivation, lack of nutrients in culture medium (starvation), or in diatoms after mutagenesis or genetic modifications, the content of FA and lipids in diatoms vary dramatically.

The results of using an alternative source of Si were published; the commonly used $Na_2SiO_3.9H_2O$ was replaced by nano-silica particles at the same concentration (Li et al., 2017). Individual diatoms behaved differently, e.g. in *Synedra* sp. the change in Si form show no effect on growth, whereas in *Navicula* sp. the addition of nano-SiO_2 resulted in a significant reduction in biomass production.

The influence of different sources of silica on the growth of three diatoms (*Cylindrotheca fusiformis*, *Navicula* sp., and *Skeletonema costatum*) was investigated; the best source of silica was quartz particles with a diameter of about 1.7 μm, but with different levels of hydrophilicity (Penna et al., 2003). The diatom *Thalassiosira pseudonana* was cultivated under silicate and nitrate starvation (Zendejas et al., 2012). The authors noted that the content of palmitic and palmitoleic acids were higher during silicate digestion, while the content of EPA was higher during nitrate starvation. Similarly, in other publications, e.g. (Adams and Bugbee, 2014; Avato et al., 1987) the effect of silica starvation on biomass and lipid production was investigated. Wei et al. (2010) reported the toxic effect of SiO_2 nanoparticles on growth of *Scenedesmus obliquus*. Their results confirm that the effect of nano-SiO_2 can have an effect on growth inhibition and pigment content. Following our earlier article (Pádrová et al., 2015) describing the effect of nano-Fe on the production of fatty acids and lipids, we focused on explaining the effect of nano-SiO_2 on the production of lipids and fatty acids in diatoms.

As in our previous publications, we used hydrophilic interaction liquid chromatography (HILIC) with high-resolution electrospray mass spectrometry in both positive and negative modes. Two fresh water diatoms (*Diadesmis gallica* and *Navicula atomus*) grown in a medium with different concentrations of nano-SiO_2 were analyzed by this method and several dozen lipid classes were identified, including PSC and SQDG, which contained several dozen molecular species of lipids. During Si starvation, the greatest changes in eicosapentaenoic acid content were found in PSC, eicosapentaenoic acid and PUFA, generally being in the *sn*-1 position.

2. Results and discussion

2.1. Production of biomass and lipids

All 3 diatom strains, i.e. strain *Navicula atomis* (CCALA 383) and strains *Diadesmis gallica* (CCALA 765 and CCALA 766), were cultured in both a medium containing 1 mM sodium metasilicate and a medium with 0.5 mM nano-SiO_2, and two diatom strains (CCALA 765 and CCALA 766) also had concentrations of 1.0 and 2.0 mM nano-SiO_2, calculated as Si. Biomass production (lyophilized cells) as well as lipid production is shown in Table 1. In both strains of *Diadesmis gallica* (strains CCALA 765 and 766), biomass and the percentage of lipids versus control (diatoms were cultured in sodium silicate) always increased, except for 2 mM nano-SiO_2, which showed a decrease. Diatoms did not grow at higher concentrations of nano-SiO_2. *Navicula atomis* (CCALA 383) did not grow at a concentration of 1 mM nano-SiO_2 in the medium. The total lipid content increased after the addition of nanoparticles, see Table 1.

Table 1
Biomass and lipid content in diatoms. The diatom strains were cultivated: *N. atomus* (383) 43 days, *D. gallica* (765) 29 days, *D. gallica* (766) 18 days.

Sample[a]	dry biomass (mg/L)[b]	lipids (%)
383 (1 mM metasilicate)	2.775 ± 0.026[c]	27.4 ± 0.20[c]
383 (0.5 mM nano-SiO_2)	2.785 ± 0.031	25.2 ± 0.17
765 (1 mM metasilicate)	2.553 ± 0.029	15.8 ± 0.24
765 (0.5 mM nano-SiO_2)	2.885 ± 0.024	18.3 ± 0.18
765 (1 mM nano-SiO_2)	2.733 ± 0.031	13.7 ± 0.22
765 (2 mM nano-SiO_2)	2.116 ± 0.025	11.9 ± 0.21
766 (1 mM metasilicate)	2.674 ± 0.027	17.7 ± 0.16
766 (0.5 mM nano-SiO_2)	2.641 ± 0.022	17.8 ± 0.19
766 (1 mM nano-SiO_2)	2.945 ± 0.028	23.8 ± 0.15
766 (2 mM nano-SiO_2)	1.839 ± 0.030	22.7 ± 0.15

[a] Both nano-SiO_2 and sodium metasilicate concentrations are reported as mM of silicone.
[b] Biomass was determined gravimetrically.
[c] Data are presented as arithmetic means from 3 measurements ± standard deviations (S. D.).

However, at a concentration of 2 mM, lipid production decreased and the yield was always lower than that of the control.

The following publications describe the effect of silica starvation on biomass and lipid production. For example, in *Cylindrotheca fusiformis,* the neutral lipid content increased more than two fold (Avato et al., 1987). Another example is the marine diatoms of *Chaetoceros gracilis* and *Thalassiosira pseudonana,* the total lipid production in the latter being 24% higher than under nitrogen limitation. The effect of silica type was tested in three marine diatoms (*Cylindrotheca fusiformis*, *Navicul*a sp., and *Skeletonema costatum*), which were cultivated in the presence of various sources of silica and found to grow better in the presence of crystalline substrates, i.e. quartz sand and/or particles (Penna et al., 2003). The influence of P and Si on the production of lipid classes in the marine diatom *Chaetoceros gracilis* was investigated (Lombardi and Wangersky, 1991). TLC/FID analysis on an Iatroscan instrument showed that the content of acetone-extractable mobile polar lipids and phospholipids decreased slightly in the silicon-starved cells. Conversely, in most diatoms, silicon is one of the key components of the cell wall structure and its lack reduces biomass production (Bozarth et al., 2009).

Zhang et al. (2018) found an overproduction of PUFA after insertion of the SOD1 gene to thraustochytrid *Schizochytrium* sp. Overexpression of the SOD1 gene resulted in attenuation of reactive oxygen species (ROS). This means that the low concentration of ROS increases the production of PUFAs, which is entirely consistent with our results, where low concentrations of nano-SiO2 create a stressful situation, probably contributing to the formation of ROS. In addition, the lack of water-soluble Si compounds induced a phenomenon similar to silica starvation. The combination of these phenomena resulted in higher biomass and lipid production and influenced changes in the representation of fatty acids and consequently lipid classes, including their molecular species (plastidial versus explastidial pathway biosynthesis of PSC).

The following findings can be drawn from the above published data and from experimental results obtained. The production of biomass and lipids is mainly influenced by strains of diatoms; see for example the various responses described in *Synedra* versus *Navicula*, or even *Navicul*a versus *Diadesmis*. The effect of the type of silicon source (Si compound), i.e. water-soluble silicate versus nano-SiO_2, was also observed and confirms that results depend on the concentration of the silicon compound in the culture medium.

The increase in lipid production by nanoparticles was effective (Table 1), however, only at lower concentrations (0.5, 1.0 and 2.0 mM), similar to sodium metasilicate (1.0 mM) in control cultures, but nano-SiO_2 suppressed cell growth at higher concentrations, i.e. above 2.0 mM. This could be related to the formation of ROS and/or aggregation of cell algae. It is also possible that the toxicity of nano-SiO_2 is manifested due to their uptake on the algal cell surface. The potential production of ROS

would correspond to increased production of eicosapentaenoic acid, which acts as an antioxidant. Nanoparticles can therefore be considered as an auxiliary tool for increasing lipid production.

2.2. Analysis of fatty acids

Fatty acids including PUFAs (Table 2) were identified by GC/MS of fatty acid methyl esters (FAME) on a polar capillary column. The positions of the double bonds were determined from the fragmentation of FAME, where an abundant ion at *m/z* 108 was formed in mass spectra of n-3 PUFA methyl esters, whereas n-6 methyl esters of PUFA produced an ion at *m/z* 150 (Fellenberg et al., 1987). The structure of PUFA was confirmed by 3-pyridylcarbinol esters (formerly called picolinyl esters). The mass spectra of these derivatives was characterized by the fact that, in addition to the ions present in all 3-pyridylcarbinol esters (ions at *m/z* 92, 108, 151 164 Da, etc.), other diagnostic ions were also present. The structure can be determined based on ions for which the interval of 14 Da (methylene group) is mistaken for the gap of 26 or 40 Da (-CH═CH- or –CH_2-CH═CH-). An example is the mass spectrum of the 3-pyridylcarbinyl ester of 20:5n-3 acid (Fig. 1). The ions at *m/z* 204, 244, 284, 324, and 364 exhibit gaps of 40 Da. Based on these values it can be clearly seen that the given mass spectrum corresponds to the structure of 3-pyridylcarbinol 5,8,11,14,17-eicosapentaenoate (20:5n-3), see also the relevant www pages (Christie). Other fatty acids were identified similarly.

The maximum lipid production was achieved at a concentration of 1 mM nano-SiO_2 in the medium. Table 2 shows the fatty acid content of diatom biomass grown under different conditions, i.e., with different sources and at different concentrations of silicon. From Fig. 2, in which 3 major FAs (palmitoleic, palmitic and eicosapentaenoic (EPA)) were selected, it is clear that with increasing nano-SiO_2 concentration, the content of palmitoleic acid initially increased and then decreased, whereas the trend with EPA was the opposite. Similar results were observed in two diatoms described in the literature (d'Ippolito et al., 2015). In *Thalassiosira weissflogii* under Si limitation, the palmitoleic acid content decreased to 75% of the control, while the EPA content increased to 131% of the control. Similarly, in *Cyclotella cryptica,* the EPA content rose to 116% of the control cultivation.

Palmitoleic acid was proven to be the major FA in all three diatom strains as well as in biomass obtained from all cultivations. Its majority representation has been previously described (Roessler, 1988; Stonik and Stonik, 2015). The change in silicon source was particularly reflected in the 20:5n-3 content, which was determined to be lower at 0.5 mM nano-silica, but up to 2 fold higher compared to the control (water-soluble sodium metasilicate). We suggest this phenomenon is due to oxidative stress to which the diatoms were exposed. A similar phenomenon has been observed previously with α-Fe_2O_3 and MgO nanoparticles (He et al., 2017). However, it should be noted that in their case, the nanoparticles caused a decrease in the production of PUFA. A similar

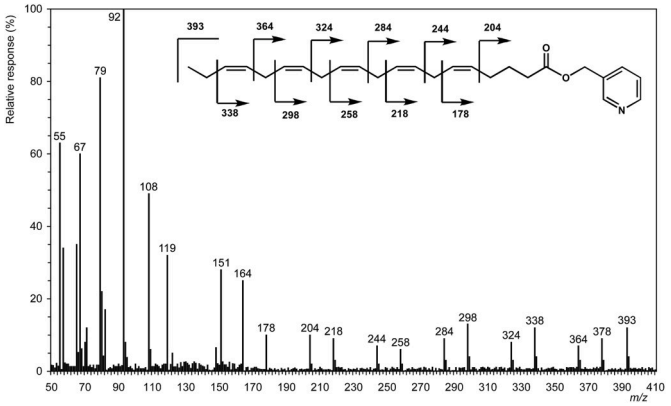

Fig. 1. Mass spectrum of the 3-pyridylcarbinyl ester of 20:5n-3 acid.

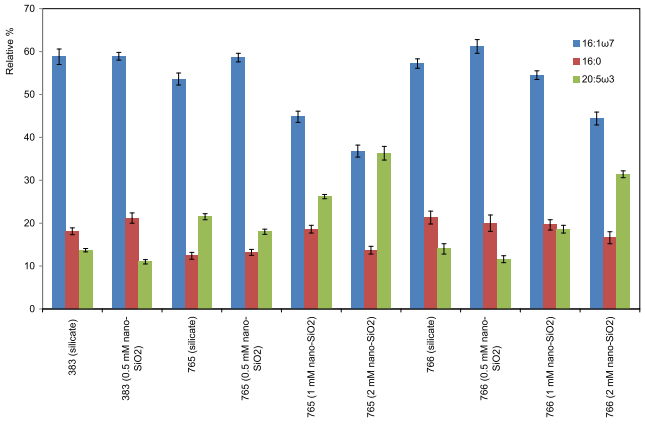

Fig. 2. Production of three major fatty acids (palmitoleic, palmitic and eicosapentaenoic acids) by 3 strain of diatoms (*Navicula atomis* (CCALA 383) and *Diadesmis gallica* (CCALA 765 and CCALA 766)) during cultivation in medium containing sodium metasilicate and/or different concentrations of nano-SiO_2. Data are presented as arithmetic means from 3 measurements ± standard deviations (S. D.).

Table 2
Fatty acid content of diatom biomass grown under different conditions.

Fatty acid	383[a] (1 mM sodium silicate)	383 (0.5 mM nano Si)	765 (1 mM sodium silicate)	765 (0.5 mM nano Si)	765 (1 mM nano Si)	765 (2 mM nano Si)	766 (1 mM sodium silicate)	766 (0.5 mM nano Si)	766 (1 mM nano Si)	766 (2 mM nano Si)
14:0	2.0 ± 0.2[b]	1.3 ± 0.2	2.7 ± 0.2	2.9 ± 0.2	2.7 ± 0.3	2.2 ± 0.3	1.3 ± 0.2	1.1 ± 0.2	1.4 ± 0.2	1.2 ± 0.2
i15:0	0.3 ± 0.1	0.2 ± 0.1	0.3 ± 0.1	0.4 ± 0.1	0.3 ± 0.1	0.3 ± 0.1	0.3 ± 0.2	0.3 ± 0.1	0.2 ± 0.1	0.4 ± 0.1
15:0	0.2 ± 0.1	0.3 ± 0.1	0.4 ± 0.1	0.2 ± 0.1	0.4 ± 0.1	0.6 ± 0.2	0.2 ± 0.1	0.3 ± 0.1	0.3 ± 0.1	0.2 ± 0.1
16:1ω7	58.8 ± 1.8	58.9 ± 0.9	53.6 ± 1.4	58.6 ± 1.0	44.8 ± 1.3	36.8 ± 1.4	57.2 ± 1.1	61.2 ± 1.6	54.5 ± 1.0	44.4 ± 1.5
16:0	18.1 ± 0.8	21.2 ± 1.2	12.4 ± 0.8	13.2 ± 0.7	18.6 ± 0.9	13.7 ± 0.9	21.3 ± 1.5	20.0 ± 1.9	19.6 ± 1.2	16.6 ± 1.4
18:3ω6	0.3 ± 0.1	0.3 ± 0.1	0.3 ± 0.1	0.2 ± 0.1	0.2 ± 0.1	0.7 ± 0.1	0.1 ± 0.1	0.2 ± 1.0	0.2 ± 0.1	0.1 ± 0.1
18:4ω6	2.9 ± 0.3	3.2 ± 0.4	2.6 ± 0.2	2.6 ± 0.2	2.2 ± 0.2	2.2 ± 0.3	2.4 ± 0.3	2.0 ± 0.2	2.9 ± 0.2	2.6 ± 0.2
18:2ω6	1.1 ± 0.2	0.8 ± 0.3	1.1 ± 0.2	0.5 ± 0.1	0.7 ± 0.2	0.8 ± 0.2	0.6 ± 0.1	0.6 ± 0.1	0.2 ± 0.1	0.6 ± 0.2
18:1ω9	0.9 ± 0.1	0.8 ± 0.2	0.8 ± 0.1	0.7 ± 0.2	0.7 ± 0.1	0.6 ± 0.2	0.6 ± 0.1	0.6 ± 0.2	0.7 ± 0.2	0.6 ± 0.1
18:1ω7	0.7 ± 0.1	0.8 ± 0.3	1.9 ± 0.3	1.0 ± 0.3	0.8 ± 0.3	3.5 ± 0.4	0.7 ± 0.2	1.0 ± 0.2	0.6 ± 0.1	0.6 ± 0.1
18:0	0.6 ± 0.1	0.6 ± 0.1	1.5 ± 0.2	1.2 ± 0.1	1.6 ± 0.1	1.7 ± 0.1	1.0 ± 0.1	0.7 ± 0.1	0.7 ± 0.1	0.6 ± 0.1
20:4ω6	0.2 ± 0.1	0.5 ± 0.1	0.3 ± 0.1	0.2 ± 0.1	0.4 ± 0.1	0.3 ± 0.1	0.0 ± 0.0	0.2 ± 0.1	0.0 ± 0.0	0.1 ± 0.1
20:5ω3	13.7 ± 0.4	11.0 ± 0.5	21.5 ± 0.7	18.0 ± 0.6	26.2 ± 0.5	36.3 ± 1.6	14.0 ± 1.2	11.6 ± 0.8	18.6 ± 0.9	31.4 ± 0.8
20:4ω3	0.2 ± 0.0	0.1 ± 0.1	0.6 ± 0.1	0.3 ± 0.2	0.4 ± 0.1	0.3 ± 0.1	0.3 ± 0.1	0.2 ± 0.1	0.1 ± 0.1	0.6 ± 0.1

[a] Strain 383 is *Navicula atomus* CCALA 383, strain 765 is *Diadesmis gallica* CCALA 765, strain 766 is *Diadesmis gallica* CCALA 766.
[b] Data are presented as arithmetic means from 3 measurements ± standard deviations (S. D.).

decrease was observed in the case of silicon-deficient cultivation medium (Roessler, 1988). The results of the analyses can be interpreted as a response to changes in membrane fluidity. PUFAs in membranes are important for adjusting to ROS-induced fluidity.

2.3. HILIC separation of lipid classes

Lipid classes were separated by HPLC, i.e. by HILIC under the conditions described previously (Rezanka et al., 2011; Vítová et al., 2016). As can be seen from Fig. 3, most lipid classes were separated on the base line, and their abundance is shown in Fig. 1S (heat maps, Supplementary data); the same applied to lipids containing a sulfur atom in the molecule. A total of 34 lipid classes were separated, of which 25 were fully characterized in less than 1-h analysis. Their structures were tentatively determined based on the characteristics of their retention times (t_R) compared with those of standards. Additional identification of lipid classes was performed by MS but only incomplete separation of molecular species within the class was achieved (Fig. 3). Therefore, single ion monitoring (SIM) was used in both negative and positive ESI to identify SQDG (at *m/z* 225.0075, i.e. $[C_6H_9O_7S]^-$) and at *m/z* 184.0733 for PSC; for the ion structure see Table 1S. The most intensive changes in the proportion of individual lipid classes were observed in lipids from our cultivations of diatoms having sulfur in the molecule, i.e. SQDG and PSC. For instance, a change in the silicon source (2 mM nano-SiO_2) increased its production of PSC up to 56% relative to the control, see below.

In addition to common lipid classes (PC, PG, PI, MGDG, DGDG, and SQDG) in the marine oleaginous diatom *Fistulifera solaris* (Liang et al., 2014), three minor and two major peaks were found but not identified by HPLC in the diatom *Navicula* cf. *perminuta* (Schaub et al., 2017). In the diatom *Phaeodactylum tricornutum*, MGDG, DGDG, SQDG, and PC were determined (Yongmanitchai and Ward, 1993) by the classical method, i.e. RP-HPLC. Polar head biosynthesis in PSC is assumed to proceed analogously to that of PC (Anderson et al., 1979). The above data suggests that our three strains (CCALA 383, 765, and 766) do not differ in their lipid composition from other diatoms. Changes in the quantitative representation of lipid classes depending on the culture conditions (sources of silica) are discussed below. Similar physical properties of PC and PSC e.g. transitional temperatures or permeability of membranes, have been described (Kates and Tremblay, 1982). Therefore, we believe that, as described for other eukaryotic cells (Liu et al., 2007), although taxonomically distant, diatoms also exhibit silica-stimulated induction of phosphatidylcholine-specific phospholipase C. This increased activity results with an up to 20 fold increase in PC content after 30 days of quartz administration, as described (Grunspan et al., 1973). Obviously, this is only one of the possible mechanisms for increasing the PSC content, since it has also been shown in organisms taxonomically very distant, but always in eukaryotic cells.

2.4. Molecular species of phospholipids

Individual fractions of lipid classes were collected and the fractions with a t_R of 23.05 min were further analyzed by flow injection analysis (FIA) in positive ESI (Fig. 4). Identification of molecular species of PSC is listed in Table 3.

Mass spectra of PSC are not measured frequently, probably due to the small distribution of these phospholipids in nature. As an isolated example, two publications describe the use of desorption chemical ionization (DCI-MS) (Bisseret et al., 1985) and field desorption (FD-MS) (Wood et al., 1980). Both ionizations belong to soft ionization and it can be assumed that spectra measured by DCI-MS, FD-MS, and ESI-MS will be similar, although not identical. The positive ion ESI of a group of peaks with a retention time of ~23.05 min is presented in Fig. 4. The MS showed that one of the major ions at *m/z* 789.5075 formed an ion $[M+Li]^+$. Both the synthesized standard (18:0/20:4-PSC), see above, and the most natural phosphatidylsulfocholines, have almost identical mass spectra, see Tables 1S and 2S

The structures shown in these tables were designed based on the similarity of PC structures previously published (Hsu and Turk, 2003, 2009bib_Hsu_and_Turk_2003bib_Hsu_and_Turk_2009) and PSC. Some of the PSC ions were structurally identical to those generated by tandem MS of the respective PC, but only when the polar moiety of the ion was cleaved. Major ions in ESI^+ are mainly those that lose a polar head, i.e. $[M + Li–S(CH_2)_2]^+$, $[M + Li–S(CH_2)_2$-ethylene phosphate$]^+$ (base peak) ions; this ion has an analogous structure to the ion of PC ($[M + Li–N(CH_3)_3$-ethylene phosphate$]^+$) arising in positive ESI, see Hsu et al. (Hsu and Turk, 2009). Furthermore, an abundant ion was present, which is believed to have the structure of $[M + Li–S(CH_2)_2–C_2H_4LiO_4P]^+$. A group of other ions arose from the loss of acyls, either as fatty acids or as ketenes, e.g. ions in Tables 1S and 2S ($[M + Li–S(CH_3)_2–C_2H_5O_4P–C_{18}H_{27}CH{=}C{=}O]^+$). We also assume that the same rule (Hsu and Turk, 2009) describing the preference of the ions in tandem MS of PC can be applied to PSC, i.e. that the loss of a carboxylic acid esterified to *sn*-1 glycerol results in a more abundant peak than that generated by cleavage of the fatty acid at the *sn*-2 position. Therefore, we assume that the representation of structures of PSC, i.e. 16:0/20:5-PSC versus 20:5/16:0-PSC is different and depends on the conditions of cultivation (the silicon source) (Fig. 5). This finding is based on the abundance of the respective ions of molecular species containing palmitic and eicosapentaenoic acids, as compared to the abundance of the respective ions of the synthetic standard 18:0/20:4-PSC. Analysis of the major molecular species, i.e.

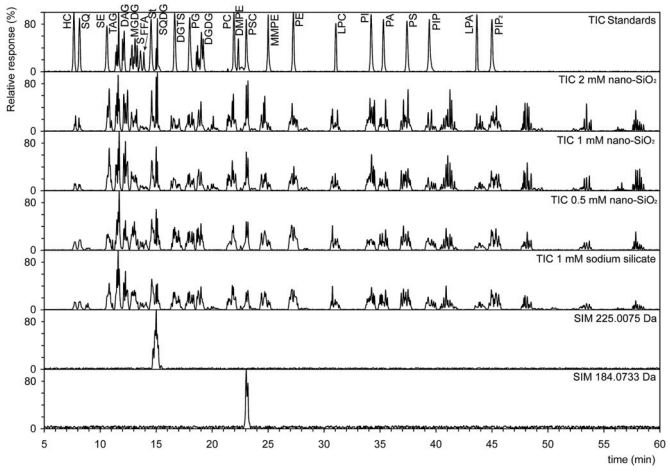

Fig. 3. Separation of lipid classes of diatom *Diadesmis gallica* (CCALA 766) by HILIC-HPLC under different modes (total ion current, single ion monitoring).

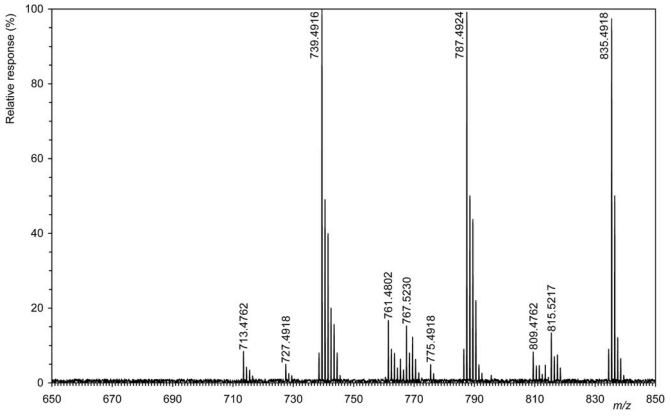

Fig. 4. Positive ion ESI of a group of peaks with a retention time of ~23.05 min (HILIC), i.e. phosphatidylsulfocholines.

Table 3
Identification of molecular species of PSC.

Molecular species	$[M+Li]^+$	mol spec1	abund1±SD[a]	mol spec2	abund2±SD	mol spec3	abund3±SD	mol spec4	abund4	sum of abund
PSC 28:0	687.4605	M/M	0.65 ± 0.18							0.65
PSC 29:0	701.4762	M/X	0.36 ± 0.11							0.36
PSC 30:1	713.4762	M/Po	8.40 ± 0.86							8.40
PSC 30:0	715.4918	M/P	3.22 ± 0.57	X/X	0.18 ± 0.07					3.40
PSC 31:1	727.4918	X/Po	4.96 ± 0.48							4.96
PSC 31:0	729.5075	X/P	1.89 ± 0.23							1.89
PSC 32:4	735.4631	M/St	0.65 ± 0.14							0.65
PSC 32:3	737.4764	M/Ln	0.31 ± 0.10							0.31
PSC 32:2	739.4916	M/L	0.33 ± 0.13	Po/Po	99.67 ± 1.67					100.00
PSC 32:1	741.5083	M/O	1.07 ± 0.22	Po/P	38.85 ± 1.03					39.92
PSC 32:0	743.5245	M/S	0.54 ± 0.09	P/P	15.06 ± 0.69					15.60
PSC 33:4	749.4762	X/St	0.36 ± 0.14							0.36
PSC 33:3	751.4918	X/Ln	0.16 ± 0.08							0.16
PSC 33:2	753.5075	X/L	0.17 ± 0.07							0.17
PSC 33:1	755.5231	X/O	0.61 ± 0.31							0.61
PSC 33:0	757.5388	X/S	0.29 ± 0.09							0.29
PSC 34:5	761.4802	M/E	8.29 ± 0.84	Po/St	8.40 ± 0.12					16.69
PSC 34:4	763.4945	M/A	0.29 ± 0.10	Po/Ln	4.43 ± 0.31	P/St	3.22 ± 0.41			7.94
PSC 34:3	765.5078	Po/L	4.70 ± 0.52	P/Ln	1.68 ± 0.17					6.38
PSC 34:2	767.5230	Po/O	13.43 ± 0.96	P/L	1.78 ± 0.24					15.21
PSC 34:1	769.5397	Po/S	7.08 ± 1.02	P/O	5.18 ± 0.33					12.26
PSC 34:0	771.5544	P/S	2.71 ± 0.57							2.71
PSC 35:5	775.4918	X/E	4.89 ± 0.69							4.89
PSC 35:4	777.5075	X/A	0.14 ± 0.07							0.14
PSC 36:8	783.4610	St/St	0.65 ± 0.26							0.65
PSC 36:7	785.4767	Ln/St	0.31 ± 0.14							0.31
PSC 36:6	787.4924	Po/E	98.68 ± 1.33	Ln/Ln	0.13 ± 0.09	St/L	0.33 ± 0.07			99.14
PSC 36:5	789.5075	Po/A	4.17 ± 0.75	P/E	38.33 ± 1.84	Ln/L	0.14 ± 0.05	St/O	1.07 ± 0.30	43.71
PSC 36:4	791.5232	P/A	1.58 ± 0.21	Ln/O	0.54 ± 0.10	St/S	0.54 ± 0.20	L/L	0.16 ± 0.08	2.82
PSC 36:3	793.5396	Ln/S	0.25 ± 0.10	L/O	0.57 ± 0.13					0.82
PSC 36:2	795.5546	L/S	0.27 ± 0.11	O/O	1.75 ± 0.09					2.02
PSC 36:1	797.5719	O/S	0.89 ± 0.26							0.89
PSC 36:0	799.5857	S/S	0.44 ± 0.14							0.44
PSC 38:9	809.4762	St/E	8.29 ± 0.83							8.29
PSC 38:8	811.4905	Ln/E	4.37 ± 0.36	St/A	0.29 ± 0.08					4.66
PSC 38:7	813.5061	Ln/A	0.12 ± 0.07	L/E	4.63 ± 0.64					4.75
PSC 38:6	815.5217	L/A	0.13 ± 0.09	O/E	13.25 ± 1.42					13.38
PSC 38:5	817.5373	O/A	0.50 ± 0.15	S/E	6.98 ± 0.63					7.48
PSC 38:4	819.5529	S/A	0.23 ± 0.10							0.23
PSC 38:10	835.4918	E/E	97.37 ± 1.29							97.37
PSC 40:9	837.5061	A/E	4.11 ± 0.35							4.11
PSC 40:8	839.5217	A/A	0.11 ± 0.07							0.11

[a] Data are presented as arithmetic means from 3 measurements ± standard deviations (S. D.).

20:5/16:0-SQDG, is described in Supplementary data, and the tandem mass spectrum is shown in Fig. 6.

It should be noted at this point that the results published so far describing esterification at *sn*-1 and/or *sn*-2 positions, i.e. positional isomers (regioisomers) of phospholipids, are not unambiguous. As can be seen from both our results and published data, the proportion of phospholipid regioisomers containing at least one PUFA in a molecule depends on the ratio of efficacies of plastidial versus explastidial pathways. Their influence will be discussed below.

The plastidial pathway uses acyl-ACP for the synthesis of PA and is similar to that found in photosynthetic prokaryotes (Lohden and Frentzen, 1988). Two enzymes are important for the biosyn thesis of PA, i.e. glycerol-3-phosphate acyltransferase and mon oacylglycerol-3-phosphate acyltransferase, as previously described (Frentzen et al., 1983). The plastidial pathway differs from the explastidial pathway by the presence of C16 fatty acids at the *sn*-2 position of the glycerol backbone. The explastidial pathway leads to the formation of two types of molecular species, one of which contains PUFAs at both glycerol positions and the other molecular species contains PUFAs at the *sn*-2 position and palmitate at the *sn*-1 position. This pathway requires collaboration between plastids and the endoplasmic reticulum in the formation of glycerolipids in chloroplasts (Roughan and Slack, 1981; Sato and Murata, 1982).

The fraction of molecular species of PC that contain C16 fatty acids at *sn*-1 are formed by the "prokaryotic or plastidial pathway". In contrast, C18 acids (synthezised by the "eukaryotic or explastidial pathway") were identified in position *sn*-2; they were gradually elongated and desaturated to form eicosapentaenoic acid (Stonik and Stonik, 2015). These reactions, including polar head exchange, are essential for the biosynthesis of phospholipids, glycolipids and TAG.

Based on tandem MS, it was found that the *sn*-2 position of major molecular species from *F. solaris*, i.e. MGDG, DGDG, SQDG, PG and PI, was preferentially esterified with C16 fatty acids. This finding also applies in part to PC and TAG. However, molecular species of PC containing PUFA, i.e. arachidonic and eicosapentaenoic acids, at the *sn*-2 position have also been identified. This suggests that both the plastidial pathway in chloroplasts and the explastidial pathway in the endoplasmatic reticulum may occur during PC biosynthesis (Liang et al., 2014).

After collection of the appropriate individual molecular species eluted from HPLC, enzymatic hydrolysis with lipase and phospholipase A_2 was used to determine the FAs at both the *sn*-1 and *sn*-2 positions in *P. tricornutum*. For example, 20:5/16:4-MGDG, 20:5/16:1-DGDG, and 16:1/16:1-SQDG were identified as the major molecular species, suggesting that, with some exceptions, PUFAs (arachidonic and eicosapentaenoic acids) were located in the *sn*-1 position (Yongmanitchai and Ward, 1993).

Liang et al. (2014) reported that "the *sn*-2 position of all chloroplast lipids and a proportion of PC species was occupied by C16 fatty acids." in marine oleaginous diatom *Fistulifera solaris*, while in another publication

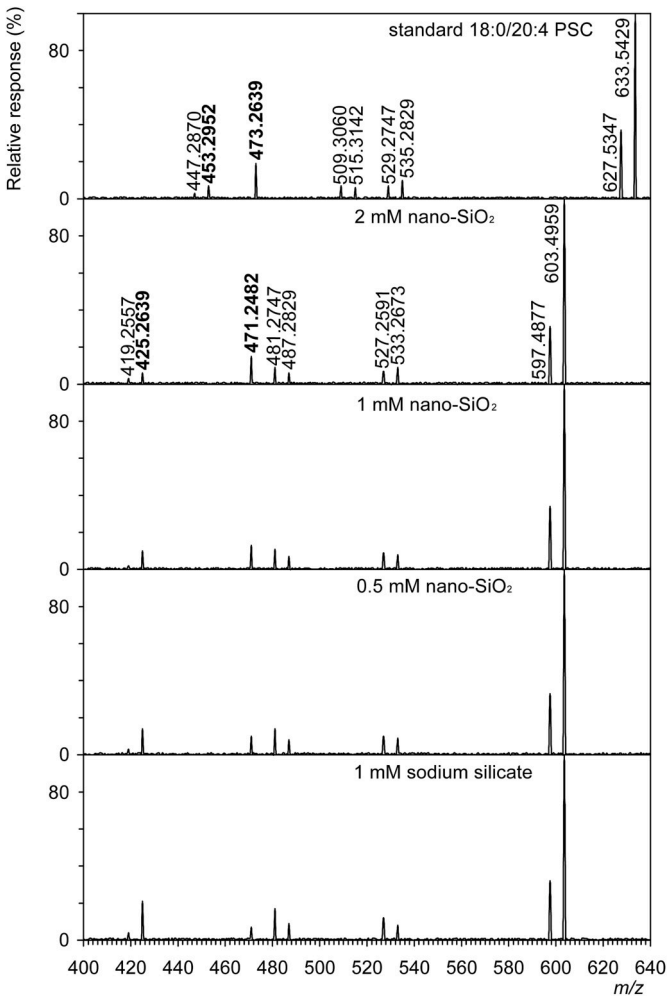

Fig. 5. Different abundancies of ions by tandem MS of molecular species of phosphatidylsulfocholine, i.e. 16:0/20:5-PSC versus 20:5/16:0-PSC under different cultivation conditions (i.e., the source of silicon).

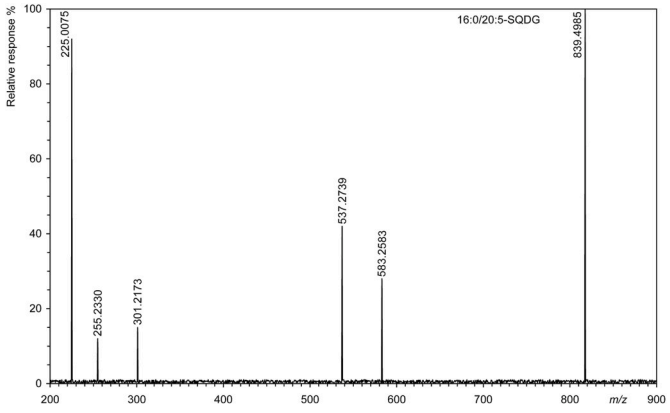

Fig. 6. Tandem mass spectrum of 16:0/20:5-SQDG (sulfoquinovosyldiacylglycerol).

(Xu et al., 2010), the authors reported that "PG and SQDG had a typical mixed biosynthetic pathway (both prokaryotic and eukaryotic pathways)" in the marine diatom *Stephanodiscus* sp.. The published results show that biosynthesis by both plastidial (in the chloroplast) and explastidial (in the endoplasmic reticulum) pathways occurs with PC and probably also PSC.

The same applies to other algae, for example, according to da Costa et al. (2019), in the brown macroalga *Fucus vesiculosus,* the galactolipid MGDG was found to contain the regioisomer 20:4/16:0 while PG contained the regioisomer 16:0/20:4. Both lipids should contain the same regioisomers, since they should be biosynthesized by the plastidial pathway.

Reverse phase HPLC of DAG, as a derivative of 3,5-dinitrophenylurethanes of the red alga *Gracilaria vermiculophylla,* made it possible to separate the molecular species of MGDG, DGDG, SQDG and PC (Honda et al., 2016). For example, it was found that the ratio of 20:4/16:0 versus 16:0/20:4 of SQDG was 58.4:0.2, while for PCs the ratio was 0.0:26.3. The results clearly indicate that while glycolipids are biosynthesized by the plastidial pathway, PC is biosynthesized by the explastidial pathway.

3. Conclusion

Diatoms were cultured both in sodium metasilicate-containing culture medium and in the presence of nano-silica (nano-SiO_2). Analysis of total lipids from three strains of diatoms *Diadesmis gallica* and *Navicula atomus* by means of HILIC-LC/high resolution ESI-tandem MS resolved 34 classes of lipids, including identification of tens of molecular species of lipids and their regioisomers. Addition of nano-SiO_2 caused an increase in the production of polyunsaturated fatty acids (PUFAs) and an increase in the production of sulfur-containing lipids, i.e. sulfoquinovosyldiacylglycerol and phosphatidylsulfocholine. A change in the representation of molecular species of phosphatidylsulfocholine (PSC)-containing fatty acids in the sn-1 versus sn-2 position was observed, which signified an effect on their biosynthesis by the plastidial rather than the explastidial pathway. These results can be used both to increase the production of PUFAs and also to prepare structured phospholipids.

4. Materials and methods

4.1. Chemical and standards

1,2-Dipalmitoyl-diacylglyceryltrimethylhomoserine (DGTS), di-all cis-4,7,10,13,16,19-docosahexaenoyl-PC, and 1,2-dioleoyl PI (ammonium salt) were purchased from Avanti Polar Lipids, Alabaster, AL, USA. DGDG, MGDG, and sulfoquinovosyldiacylglycerol (SQDG) (plant leaf lipids), cholesteryl linoleate, 1,2-di-all cis-4,7,10,13,16,19-docosahexaenoin, 1,2-dioleoyl- phosphatidic acid (PA), 1,2-dioleoyl-PC, 1,2-dioleoyl-PE, 1,2-dioleoyl-phosphatidylglycerol (PG) (Na-salt), tri-all cis-4,7,10,13,16,19-docosahexaenoin, and 1,2-dimyristoyl-phosphatidylserine (PS) (Na-salt) from Larodan (Malmo, Sweden). All other chemicals were purchased from Sigma-Aldrich (Prague, CR). Silica nanoparticles (nano-SiO_2, average diameter 10 nm) were purchased from Cabot (Leuven, Belgium).

4.2. Cultivation of microalgal strains

The diatoms *Navicula atomus* (Kützing) Grunow (CCALA 383) (class Bacillariophyceae, order Naviculales, family Naviculaceae) and two strains of *Diadesmis gallica* W. Smith (CCALA 765 and CCALA 766) (class Bacillariophyceae, order Naviculales, family Diadesmidaceae) were purchased from the Culture Collection of Autotrophic Organisms (CCALA) at the Institute of Botany, the Czech Academy of Sciences, Třeboň, Czech Republic.

The strains were cultivated under the laboratory conditions in units consisting of glass cylinders (V = 300 mL) in a water bath (15 °C), and continuously illuminated by a panel of dimmable fluorescent lamps (DULUX L55W/950 Daylight, OSRAM, Milano, Italy) with an incident light intensity of 300 μmol m^2 s^{-1}. The cultures were aerated with air containing 2% (v/v) carbon dioxide. Silicon was added either in the form of a solution of sodium metasilicate nonahydrate - Na_2SiO_3 . $9H_2O$ (control cultures, final concentration 1 mM) or as nano-SiO_2 to the mineral medium used for experimental cultures (Vítová et al., 2011).

The strains were cultivated until the control cultures reached the Abs_{750} = 1.00, *N. atomus* 43 days, *D. gallica* (765) 29 days and *D. gallica* (766) 18 days.

The nano-SiO_2 was resuspended in distilled water (1.16 g/20 mL) and sonicated using a SONOPULS, (BANDELIN electronics, Berlin, Germany) for 1 min, at 40%. Strains were inoculated at Abs_{750} = 0.02. Water glass (1 mL/100 mL) was added to each control culture and nano-SiO_2 was added to each strain to achieve final sodium metasilicate nonahydrate concentrations of 0.5 mM, 1 mM and 2 mM. The strains were not able to grow without addition of silicate, thus this type of control culture was not included in the experimental design.

4.3. Synthesis of 1-stearoyl-2-arachidonoyl-sn-3-phosphatidyl sulfocholine

Synthesis of 18:0/20:4-PSC is fully described in the Supplementary data.

4.4. Isolation of lipids

Isolation and pretreatment of lipids was carried out according to Bligh and Dyer (1959), with modifications as described previously (Kates and Volcani, 1966). For full description of the experiments see the Supplementary data.

4.5. FAME and 3-pyridylcarbinol esters analysis

Analysis of fatty acids in the form of methyl esters (FAME) was described previously (Rezanka, 1990; Vancura et al., 1988) A complete description of all conditions of FAME and 3-pyridylcarbinol esters analysis by GC-MS is in the Supplementary data.

4.6. HILIC/MS-ESI

After purification by Sep-Pak Vac Silica cartridge (Waters Gesellschaft m.b.H., Czech Republic), the lipids were identified and quantified by LC/MS. A detailed description of both positive and negative ion ESI is again in the Supplementary data.

4.7. Statistical analysis

The statistical analysis was performed using the IBM SPSS Statistics (Statistical Package for the Social Sciences; IBM Corp, 2013) Statistics software, version 26 (IBM® Corporation, Armonk, NY, USA), to explore the metabolic relationships between control and treated cultivations.

Declaration of competing interest

The authors declare no conflict of interest. All authors reviewed the results and approved the manuscript. All authors approved the final version to be submitted.

Statement of informed consent, human/animal rights

No conflicts, informed consent, or human or animal rights are applicable to this study.

Declaration of competing interest

The authors declare that they have no known competing financial interests or personal relationships that could have appeared to influence the work reported in this paper.

CRediT authorship contribution statement

Tomáš Řezanka: Formal analysis, Writing - original draft. **Michal Řezanka:** Writing - original draft. **Dana Mezricky:** Data curation, Formal analysis, Funding acquisition, Methodology. **Milada Vítová:** Formal analysis, Funding acquisition, Methodology, Project administration.

Acknowledgements

This research was supported by the program Interreg V-A: grant REEgain ATCZ172, by the Ministry of Education, Youth and Sports of the Czech Republic and the European Union - European Structural and Investment Funds in the framework of the Operational Programme Research, Development and Education - project Hybrid Materials for Hierarchical Structures, grant number CZ.02.1.01/0.0/0.0/16_019/0000843. We acknowledge prof. J. D. Brooker for critical reading and language editing of the text.

Appendix A. Supplementary data

Supplementary data to this article can be found online at https://doi.org/10.1016/j.phytochem.2020.112452.

References

Adams, C., Bugbee, B., 2014. Enhancing lipid production of the marine diatom *Chaetoceros gracilis*: synergistic interactions of sodium chloride and silicon. J. Appl. Phycol. 26, 1351–1357.

Anderson, R., Kates, M., Volcani, B.E., 1979. Studies on the biosynthesis of sulfolipids in the diatom *Nitzschia alba*. Biochim. Biophys. Acta 573, 557–561.

Anisimov, V.N., Zabezhinski, M.A., Popovich, I.G., Piskunova, T.S., Semenchenko, A.V., Tyndyk, M.L., Yurova, M.N., Rosenfeld, S.V., Blagosklonny, M.V., 2011. Rapamycin increases lifespan and inhibits spontaneous tumorigenesis in inbred female mice. Cell Cycle 10, 4230–4236.

Avato, P., Bianchi, G., Salamini, F., 1987. Ontogenetic variations in the chemical composition of maize surface. In: Stumpf, P.K., Mudd, J.B., Nes, W.D. (Eds.), The Metabolism, Structure, and Function of Plant Lipids. Plenum Press, pp. 549–559.

Bell, E.M., Lin, W.-c., Husbands, A.Y., Yu, L., Jaganatha, V., Jablonska, B., Mangeon, A., Neff, M.M., Girke, T., Springer, P.S., 2012. Arabidopsis lateral organ boundaries negatively regulates brassinosteroid accumulation to limit growth in organ boundaries. Proc. Natl. Acad. Sci. Unit. States Am. 109, 21146–21151.

Bisseret, P., Ito, S., Tremblay, P.A., Volcani, B.E., Dessort, D., Kates, M., 1984. Occurrence of phosphatidylsulfocholine, the sulfonium analog of phosphatidylcholine in some diatoms and algae. Biochim. Biophys. Acta 796, 320–327.

Bisseret, P., Dessort, D., Nakatani, Y., Kates, M., 1985. Ammonia desorption chemical ionization mass-spectrometry of phosphatidylsulfocholine-phosphatidylcholine mixtures. Chem. Phys. Lipids 36, 309–318.

Bligh, E.G., Dyer, W.J., 1959. A rapid method of total lipid extraction and purification. Can. J. Biochem. Physiol. 37, 911–917.

Bozarth, A., Maier, U.G., Zauner, S., 2009. Diatoms in biotechnology: modern tools and applications. Appl. Microbiol. Biotechnol. 82, 195–201.

Cramer, G.R., Urano, K., Delrot, S., Pezzotti, M., Shinozaki, K., 2011. Effects of abiotic stress on plants: a systems biology perspective. BMC Plant Biol. 11.

d'Ippolito, G., Sardo, A., Paris, D., Vella, F.M., Adelfi, M.G., Botte, P., Gallo, C., Fontana, A., 2015. Potential of lipid metabolism in marine diatoms for biofuel production. Biotechnol. Biofuels 8.

da Costa, E., Domingues, P., Melo, T., Coelho, E., Pereira, R., Calado, R., Abreu, M.H., Domingues, M.R., 2019. Lipidomic signatures reveal seasonal shifts on the relative abundance of high-valued lipids from the brown algae *Fucus vesiculosus*. Mar. Drugs 17.

Fellenberg, A.J., Johnson, D.W., Poulos, A., Sharp, P., 1987. Simple mass-spectrometric differentiation of the normal-3, normal-6 and normal-9 series of methylene interrupted polyenoic acids. Biomed. Environ. Mass Spectrom. 14, 127–129.

Frentzen, M., Heinz, E., Mckeon, T.A., Stumpf, P.K., 1983. Specificities and selectivities of glycerol-3-phosphate acyltransferase and monoacylglycerol-3-phosphate acyltransferase from pea and spinach chloroplasts. Eur. J. Biochem. 129, 629–636.

Grunspan, M., Antweiler, H., Dehnen, W., 1973. Effect of silica on phospholipids in rat lung. Br. J. Ind. Med. 30, 74–77.

He, M., Yan, Y., Pei, F., Wu, M., Gebreluel, T., Zou, S., Wang, C., 2017. Improvement on lipid production by *Scenedesmus obliquus* triggered by low dose exposure to nanoparticles. Sci. Rep. 7, 15526.

Honda, M., Ishimaru, T., Itabashi, Y., 2016. Lipid classes, fatty acid composition, and glycerolipid molecular species of the red alga *Gracilaria vermiculophylla*, a prostaglandin-producing seaweed. J. Oleo Sci. 65, 723–732.

Hsu, F.F., Turk, J., 2003. Electrospray ionization/tandem quadrupole mass spectrometric studies on phosphatidylcholines: the fragmentation processes. J. Am. Soc. Mass Spectrom. 14, 352–363.

Hsu, F.F., Turk, J., 2009. Electrospray ionization with low-energy collisionally activated dissociation tandem mass spectrometry of glycerophospholipids: mechanisms of fragmentation and structural characterization. J. Chromatogr. B 877, 2673–2695.

Kates, M., Tremblay, P.A., 1982. Can phosphatidyl sulfocholine, the sulfonium analog of lecithin, efficiently replace lecithin in natural membranes? Rev. Canad. Biol. 40, 343–349.
Kates, M., Volcani, B.E., 1966. Lipid components of diatoms. Biochim. Biophys. Acta 116, 264–278.
Lang, I., Hodac, L., Friedl, T., Feussner, I., 2011. Fatty acid profiles and their distribution patterns in microalgae: a comprehensive analysis of more than 2000 strains from the SAG culture collection. BMC Plant Biol. 11, 124.
Li, X.-I., Marella, T.K., Tao, L., Li, R., Tiwari, A., Li, G., 2017. Optimization of growth conditions and fatty acid analysis for three freshwater diatom isolates. Phycol. Res. 65, 177–187.
Liang, Y., Maeda, Y., Yoshino, T., Matsumoto, M., Tanaka, T., 2014. Profiling of polar lipids in marine oleaginous diatom *Fistulifera solaris* JPCC DA0580: prediction of the potential mechanism for eicosapentaenoic acid-incorporation into triacylglycerol. Mar. Drugs 12, 3218–3230.
Liu, H.L., Zhang, H.Q., Forman, H.J., 2007. Silica induces macrophage cytokines through phosphatidylcholine-specific phospholipase C with hydrogen peroxide. Am. J. Resp. Cell Mol. 36, 594–599.
Lohden, I., Frentzen, M., 1988. Role of plastidial acyl-acyl carrier protein - glycerol 3-phosphate acyltransferase and acyl-acyl carrier protein hydrolase in channeling the acyl flux through the prokaryotic and eukaryotic pathway. Planta 176, 506–512.
Lombardi, A.T., Wangersky, P.J., 1991. Influence of phosphorus and silicon on lipid class production by the marine diatom *Chaetoceros gracilis* grown in turbidostat cage cultures. Mar. Ecol. Prog. Ser. 77, 39–47.
Pádrová, K., Lukavský, J., Nedbalová, L., Čejková, A., Cajthaml, T., Sigler, K., Vítová, M., Řezanka, T., 2015. Trace concentrations of iron nanoparticles cause overproduction of biomass and lipids during cultivation of cyanobacteria and microalgae. J. Appl. Phycol. 27, 1443–1451.
Penna, A., Magnani, M., Fenoglio, I., Fubini, B., Cerrano, C., Giovine, M., Bavestrello, G., 2003. Marine diatom growth on different forms of particulate silica: evidence of cell/particle interaction. Aquat. Microb. Ecol. 32, 299–306.
Popovich, C.A., Damiani, C., Constenla, D., Leonardi, P., 2012. Lipid quality of the diatoms *Skeletonema costatum* and *Navicula gregaria* from the South Atlantic Coast (Argentina): evaluation of its suitability as biodiesel feedstock. J. Appl. Phycol. 24, 1–10.
Rezanka, T., 1990. Identification of very long polyenoic acids as picolinyl esters by Ag+ ion-exchange high-performance liquid-chromatography, reversed-phase high-performance liquid-chromatography and gas-chromatography mass-spectrometry. J. Chromatogr. 513, 344–348.
Rezanka, T., Siristova, L., Matoulkova, D., Sigler, K., 2011. Hydrophilic interaction liquid chromatography: ESI–MS/MS of plasmalogen phospholipids from *Pectinatus* bacterium. Lipids 46, 765–780.
Roessler, P.G., 1988. Effects of silicon deficiency on lipid-composition and metabolism in the diatom *Cyclotella cryptica*. J. Phycol. 24, 394–400.
Roughan, P.G., Slack, C.R., 1981. Acyl-coa may be a neglected product in studies of fatty-acid synthesis by isolated chloroplasts. FEBS Lett. 135, 182–186.
Sato, N., Murata, N., 1982. Lipid biosynthesis in the blue-green alga, *Anabaena variabilis* 2. fatty-acids and lipid molecular species. Biochim. Biophys. Acta 710, 279–289.
Schaub, I., Wagner, H., Graeve, M., Karsten, U., 2017. Effects of prolonged darkness and temperature on the lipid metabolism in the benthic diatom *Navicula perminuta* from the Arctic Adventfjorden. Svalbard. Polar Biol. 40, 1425–1439.
Stonik, V., Stonik, I., 2015. Low-molecular-weight metabolites from diatoms: structures, biological roles and biosynthesis. Mar. Drugs 13, 3672–3709.
Taguchi, S., Hirata, J.A., Laws, E.A., 1987. Silicate deficiency and lipid-synthesis of marine diatoms. J. Phycol. 23, 260–267.
Vancura, A., Rezanka, T., Marslalek, J., Melzoch, K., Basarova, G., Kristan, V., 1988. Metabolism of L-threonine and fatty-acids and tylosin biosynthesis in *Streptomyces fradiae*. FEMS Microbiol. Lett. 49, 411–415.
Vítová, M., Bišová, K., Hlavová, M., Zachleder, V., Rucki, M., Čížková, 2011. Glutathione peroxidase activity in the selenium-treated alga *Scenedesmus quadricauda*. Aquat. Toxicol. 102, 87–94.
Vítová, M., Goecke, F., Sigler, K., Řezanka, T., 2016. Lipidomic analysis of the extremophilic red alga *Galdieria sulphuraria* in response to changes in pH. Algal Res 13, 218–226.
Wei, C., Zhang, Y., Guo, J., Han, B., Yang, X., Yuan, J., 2010. Effects of silica nanoparticles on growth and photosynthetic pigment contents of *Scenedesmus obliquus*. J. Environ. Sci. 22, 155–160.
Wood, G.W., Tremblay, P.-A., Kates, M., 1980. Field desorption mass spectrometry of phospholipids IV-spectra of synthetic phosphatidylsulfocholinest. Biomed. Mass Spectrom. 7, 11–12.
Xu, J., Chen, D., Yan, X., Chen, J., Zhou, C., 2010. Global characterization of the photosynthetic glycerolipids from a marine diatom *Stephanodiscus* sp. by ultra performance liquid chromatography coupled with electrospray ionization-quadrupole-time of flight mass spectrometry. Anal. Chim. Acta 663, 60–68.
Yongmanitchai, W., Ward, O.P., 1993. Positional distribution of fatty-acids, and molecular-species of polar lipids, in the diatom *Phaeodactylum tricornutum*. J. Gen. Microbiol. 139, 465–472.
Zendejas, F.J., Benke, P.I., Lane, P.D., Simmons, B.A., Lane, T.W., 2012. Characterization of the acylglycerols and resulting biodiesel derived from vegetable oil and microalgae (*Thalassiosira pseudonana* and *Phaeodactylum tricornutum*). Biotechnol. Bioeng. 109, 1146–1154.
Zhang, S., He, Y., Sen, B., Chen, X., Xie, Y., Keasling, J.D., Wang, G., 2018. Alleviation of reactive oxygen species enhances PUFA accumulation in *Schizochytrium* sp. through regulating genes involved in lipid metabolism. Metab. Eng. Commun. 27, 39–48.